

## Supplementary Information

### Revealing the nitrogen reaction pathway for the catalytic oxidative denitrification of fuels

Michael Huber,<sup>a</sup> Maximilian J. Poller,<sup>a</sup> Jens Tochtermann<sup>b</sup>, Wolfgang Korth<sup>b</sup>, Andreas Jess<sup>b</sup> Jakob Albert<sup>\*a</sup>

<sup>a</sup> Institute of Technical and Macromolecular Chemistry, Hamburg University, Bundesstraße 45, 20146 Hamburg, Germany

<sup>b</sup> Chair of Chemical Engineering, Center of Energy Technology (ZET), University of Bayreuth, Universitätsstraße 30, 95447 Bayreuth, Germany

### Contents

1. General experimental information
  - a. Materials
  - b. Experimental setup & work procedure
  - c. Analytical Methods
2. Experimental Data
3. References

## General experimental Information

### Materials:

All chemicals were obtained commercially and used without further purification unless otherwise stated.

Quinaldine was purchased from Thermo Fisher Scientific with a purity of 96 %. Quinoline was purchased from Sigma-Aldrich with a purity of 98 %. Thiophene was purchased from Thermo Fisher Scientific with a purity of 99 %. 2,2,4-Trimethylpentane was purchased from Acros Organics with a purity of 99.5 %. *trans*-Decahydronaphthalene was purchased from Merck KGaA with a purity of 96.5 %. Sodium nitrate was purchased from Grüssing with a purity of 99 %. *n*-Pentane was purchased from Grüssing with a purity of 99 %. Liquid nitrogen was obtained from Linde with a purity of 99.999 %. Gaseous N<sub>2</sub> was obtained from Linde with a purity of 99.999 %. Gaseous O<sub>2</sub> was obtained from Westfalen AG with a purity of 99.999 %. The helium for the Micro-GC was obtained from Linde with a purity of 99.9999 % and the helium for the GC-MS was obtained from Linde with a purity of 99.999 %.

### Catalyst Preparation:

The HPA-5 catalyst H<sub>8</sub>PV<sub>5</sub>Mo<sub>7</sub>O<sub>40</sub> was synthesized according to the following procedure.<sup>1,2</sup> Two solutions are required for the synthesis of HPA-5. In solution 1, water (707.9 mL) is mixed with molybdenum trioxide (62.8 g) and a 25 % phosphoric acid solution (24.4 g) and boiled under reflux until a clear yellow solution is formed. For solution 2, divanadium pentoxide (28.3 g) is mixed with water (1066.7 mL). Next, the suspension is cooled to 0 °C using an ice bath. A 30 % hydrogen peroxide solution (189.5 mL) is then slowly added to the cooled suspension while stirring. During this process, divanadium pentoxide begins to dissolve, releasing oxygen gas. A 25 % phosphoric acid solution (4.2 mL) is afterwards added to the obtained red/brown solution and afterwards warmed to room temperature. Next, solution 2 is slowly added dropwise to solution 1, which still boils under reflux. The mixture turns orange/brown during this process. After adding solution 2, the mixture keeps boiling under reflux for another 1 h. Finally, the mixture is cooled to room temperature and then filtered. The water of the filtrate is removed using the rotary evaporator, leaving a brown solid.

The identity of the catalyst was confirmed by inductively coupled plasma optical emission spectroscopy (ICP-OES) (38.2 wt-% Mo, 14.8 wt-% V, 2.3 wt-% P) and ATR-FT-IR-spectroscopy (Figure S1). The phosphorus-oxygen vibration can be assigned to the bands in the region of ca. 1050 cm<sup>-1</sup>. The terminal metal-oxygen bonds refer to the vibrational bands between 950-1000 cm<sup>-1</sup>. The bridging metal-oxygen-metal bonds at the corner belong to the bands between 850-900 cm<sup>-1</sup>, while the bonds from the edge belong to the bands below 800 cm<sup>-1</sup>.<sup>3-5</sup>

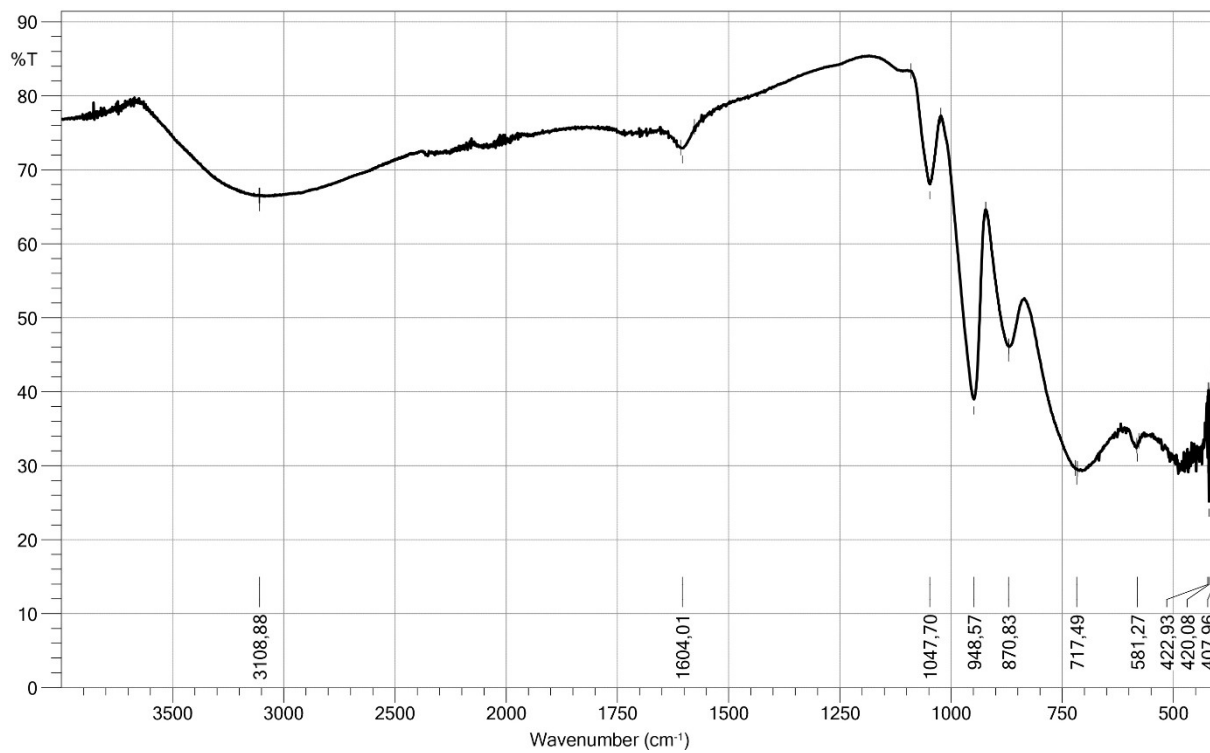


Figure S1: IR spectrum of HPA-5 powder.

## Experimental setup & work procedure

Unless otherwise stated, all tests were performed according to these standard instructions. The reactions were carried out in a 600 mL Hastelloy (C-276) autoclave with gas entrainment impeller. 200 mL deionized water containing 0.2 mmol of the catalyst and 20 mL of the model oil (2,2,4-trimethylpentane) containing the reactant and the *trans*-Decahydronaphthalene (internal standard) were charged into the vessel. For the experiments with 100 % O<sub>2</sub>, the reactor was flushed three times with 30 bar of O<sub>2</sub> to remove the air from the gas phase. Afterwards, 15 bar of O<sub>2</sub> were filled into the reactor for the heating process. Thereafter, the stirring speed was adjusted to 300 rpm and the reactor was heated to reaction temperature. When the desired reaction temperature was reached, the O<sub>2</sub> pressure was increased to 20 bar and the stirring speed was increased to 1000 rpm, which marks the start of the reaction. After the reaction the gas phase was analyzed using heated online sampling with a Micro-GC (see below for details). After the desired reaction time, the reaction was stopped by setting the stirrer speed to 300 rpm and removing the heating sleeve. Unless otherwise stated, the aqueous and organic phases were sampled after the system had reached room temperature.

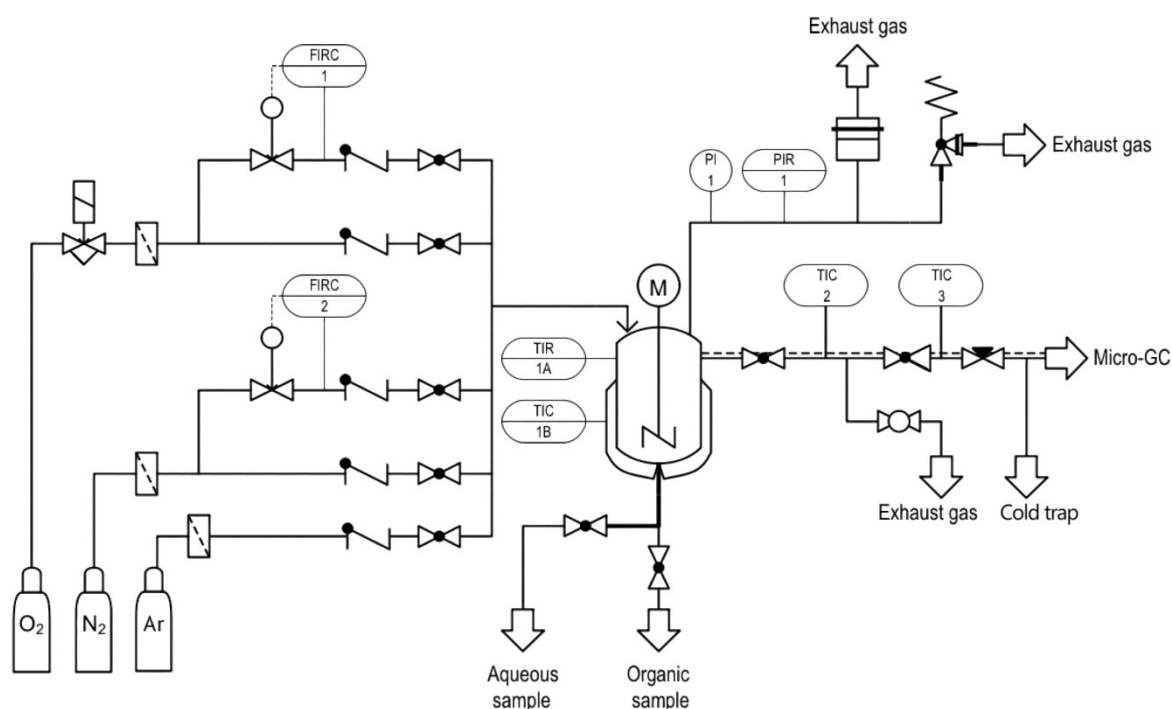


Figure S2: Schematic representation of the reactor setup.

## Analytical Methods

The organic phase was analyzed with a gas chromatograph-mass spectrometer (GC-MS) on an *Agilent 8860 GC System* with a DB-WAX Ultra Inert column (30 m length, 0.25 mm diameter, 0.25  $\mu\text{m}$  film thickness) using an Agilent 5977B GC/MSD as detector. Gas chromatography of the gaseous phase was conducted at 1 bar on a 2-module Micro-GC Fusion from *INFICON Holding AG*. The Micro-GC samples are split and measured on two columns. Module A uses a 5  $\text{\AA}$  molecular sieve column with a cross-section of 0.25 mm and a length of 10 m. A backflush with 1.0  $\mu\text{L}$  is also preceded. Module B uses a Rt-Q-Bond column with a cross-section of 0.25 mm and a length of 8 m. Each module is connected with a thermal conductivity detector (TCD). The catalyst components in aqueous phase were analyzed with an ICP-OES spectrometer, *Fa. Spectro Ametek Model Arcos*. Samples were measured without digestion at a 1:100 dilution. Additionally, the catalyst powder was analyzed by a FT-IR spectrometer using an attenuated total reflection (ATR) measurement mode on a QATR™-S single-reflection ATR (with a diamond prism) from Shimadzu. The analyses of the aqueous phase were carried out using a high-performance liquid chromatography (HPLC) system from *SHIMADZU* equipped with an Aminex HPX-87 H 300 mm  $\times$  7.8 mm *BIORAD* Column and a refractive index detector. 5 mm of an aqueous sulfuric acid solution was used as eluent. Elemental CHNS analysis of the organic phase were performed with an analyzer of *Fa. EuroVector, Model EA-3000*. Oxygen in the organic phase was measured with an Oxygen- Analyzer, *Fa. HekaTech* high temperature pyrolysis furnace. The preparation of the samples for ion chromatography (IC), where the catalyst is separated, was carried out with membrane separation. The membrane separation experiments were performed with 3" MiniMem membrane cell from PS Prozesstechnik GmbH equipped with a DK series membrane-type obtained from GE Power water & Process technologies in a self-designed experimental setup. The active membrane area is greater than 30  $\text{cm}^2$ .<sup>6</sup> The nitrate concentrations in the aqueous phase were determined by IC, *Fa. Thermo, Model Integrion* equipped with analytical column Dionex Ion Pac AS11-HC 2\*250 mm; front column Ion Pac AG11-HC 2\*50 mm. Samples were measured with a 1:500 dilution for acetate or diluted 1:1000 as well as 1:500 for formate and the values were averaged.

## Experimental Data

Table S1: CHNSO and ICP-OES measurements of the precipitate from the long-term experiment (73 h) for the conversion of 4.6 mmol of quinaldine.

	<b>Solid composition</b>	<b>Organic solid without catalyst</b>	<b>Quinaldine (substrate)</b>
C-content (%)	50.9	59.2	85.0
H-content (%)	2.9	3.4	4.0
N-content (%)	6.5	7.6	11.0
O-content (%)	25.7	29.9	0.0
V-content (%)	1.5	-	-
Mo-content (%)	4.4	-	-
P-content (%)	0.4	-	-

Table S1 presents the CHNSO and ICP-OES measurements of the solid precipitate. In addition to the oxidized quinaldine, this precipitation also contains a small proportion of the catalyst that has been precipitated with the substrate. The amount of catalyst was subtracted, based on vanadium, to maintain the pure composition of the organic solid. The mass fraction of the solid indicates that it consists of a mixture of different oxidation products from quinaldine. According to the literature, it consists of 5,8-quinaldinedione<sup>7</sup> among others.

Table S2: Micro-GC measurement of the gas phase and the yield based on carbon or nitrogen.

<b>Substance</b>	<b>Measurement (mol-%)</b>	<b>Yield (%)</b>
CO <sub>2</sub>	12.9	63.0
CO	0.5	2.3
N <sub>2</sub>	1.0	93.1

Table S2 presents the Micro-GC measurements of the gas phase. The yield of CO<sub>2</sub> and CO is normalized to the amount of carbon. That means that 63.0 % of the carbon from quinaldine has become CO<sub>2</sub> and 2.3 % has become CO. Similarly, in the case of nitrogen yield, 93.1 % of the nitrogen atom from quinaldine has become N<sub>2</sub>.

Table S3: HPLC measurement of the aqueous phase and the yield based on carbon.

<b>Substance</b>	<b>Measurement (mol/L)</b>	<b>Yield (%)</b>
Formic acid	0.017	7.3
Acetic acid	0.011	9.5
Acetone	0.007	9.1

Table S3 presents the HPLC measurements of the aqueous phase. The yield is normalized to the amount of carbon. That means that 7.3 % of the carbon from quinaldine has become formic acid, 9.5 % acetic acid and 9.1 % has become acetone.

## References

- 1 E. G. Zhizhina and V. F. Odyakov, *Reaction Kinetics and Catalysis Letters*, 2008, **95**, 301-312.
- 2 J. Albert, D. Lüders, A. Bösmann, D. M. Guldi and P. Wasserscheid, *Green Chemistry*, 2014, **16**, 226-237.
- 3 A. J. Bridgeman, *Chemistry - A European Journal*, 2004, **10**, 2935-2941.
- 4 J. K. Lee, J. Melsheimer, S. Berndt, G. Mestl, R. Schlögl and K. Köhler, *Applied Catalysis A: General*, 2001, **214**, 125-148.
- 5 J. C. Raabe, J. Albert and M. J. Poller, *Chemistry - A European Journal*, 2022, **28**, e202201084.
- 6 T. Esser, M. Huber, D. Voß and J. Albert, *Chemical Engineering Research and Design*, 2022, **185**, 37-50.
- 7 B. Bertleff, M. S. Haider, J. Claußnitzer, W. Korth, P. Wasserscheid, A. Jess and J. Albert, *Energy & Fuels*, 2020, **34**, 8099-8109.